

Drying shrinkage of alkali-activated slag and fly ash concrete; A comparative study with ordinary Portland cement concrete

Zhenming Li ¹, Jiahua Liu ², and Guang Ye ¹

¹ Delft University of Technology, the Netherlands

² Jiangsu College of Engineering and Technology, China

This study investigates the drying shrinkage and the shrinkage-induced stress of alkali-activated blast furnace slag and fly ash concrete (AC) in comparison with ordinary Portland cement concrete (OC). For samples that were dried from 1 day after casting, the drying shrinkage of AC was much higher than that of OC. For samples that were stored in a sealed condition for 28 days before drying, the subsequent drying shrinkage amplitudes of AC and OC were comparable. In both conditions, the stresses generated in AC were higher than in OC at the beginning, but experienced great reductions after certain ages, reaching less than one-fourth of the stresses in OC in the end. The stresses decrease, i.e. relaxation in AC was attributed to the pronounced non-elastic deformability of CASH gels. The non-elastic deformability of AC reduced the risk of thorough cracking, but maybe at the expense of the development of local microcracks. It is recommended to protect AC from drying at an early age to avoid micro and macrocracking.

Key words: Shrinkage, alkali-activated slag and fly ash, concrete, stress, cracking, drying

1 Introduction

Alkali-activated materials (AAMs) have emerged as eco-friendly alternatives to ordinary Portland cement (OPC). While OPC has been widely used for centuries with stable engineering performances, the cement production contributes at least 5-8% of the total CO₂ emission worldwide (Scrivener and Kirkpatrick 2008). AAMs, in contrast, are mainly made from industrial by-products or other inexpensive aluminosilicate materials, to which little or no environmental footprint is usually attributed (Provis 2014). Alkali-activated ground granulated blast furnace slag and fly ash (AASF), as an example, has attracted increasing academic and commercial interest in last decades due to not only the potential to utilize slag and fly ash but also the good engineering performances of this kind of material, such

as high strength, good chemical durability and fire resistance (Arbi et al. 2016; Juenger et al. 2011; Provis and Deventer 2009). However, several disadvantageous properties hamper a wider application of AASF, one of which is the high drying shrinkage (Cartwright, Rajabipour, and Radli 2014; Collins and J. . Sanjayan 2000). In this study, the drying shrinkage of alkali-activated slag and fly ash concrete (AC) was measured in comparison with ordinary Portland cement concrete (OC). Ring tests were performed to characterize the cracking potential and shrinkage-induced stress of the two concretes in a restraint condition (See, Attiogbe, and Miltenberger 2003). In this paper, the mechanisms behind the drying shrinkage and the stress development in AC are also discussed.

2 Materials and experiments

2.1 Materials

The precursors used for preparation of AC were ground granulated blast furnace slag (GGBFS) and fly ash (FA). GGBFS had a specific gravity of 2890 kg/m³, while FA had a specific gravity of 2440 kg/m³. The chemical compositions of the precursors are given in Table 1. The amorphous phase was dominant in GGBFS as reported in a previous study (Nedeljković, Li, and Ye 2018). In contrast to GGBFS, FA contained beside amorphous also crystalline phases such as mullite, quartz and hematite (Nedeljković et al. 2018). The precursors were activated by sodium hydroxide and sodium silicate. The composition of the alkaline activator was set according to recommendations from earlier studies (Burciaga-Díaz et al. 2010; Douglas et al. 1991; Wang, Scrivener, and Pratt 1994). The alkaline activator was prepared by mixing sodium hydroxide pellets (analytical grade, >98 % purity) with distilled water and sodium silicate solution (Na₂O: 8.25 wt. %, SiO₂: 27.50 wt. %). The solutions were then allowed to cool for 24 hours before sample preparation. CEM I 52.5 N cement was used to prepare OC. CEM I 52.5 N had a specific gravity of 3.15 kg/m³. The chemical composition of cement is also shown in Table 1.

Detailed mixture designs of AC and OC are given in Table 2. It should be noted that the specific proportions of the aggregates were not exactly the same to obtain good workability of both concrete, but the volume ratios of binder/concrete in these two concretes were kept rather similar at around 30%, to eliminate the influence of binder content on the shrinkage properties.

Table 1: Chemical compositions of FA, GGBFS and OPC measured with X-ray fluorescence

Oxide (%)	SiO ₂	Al ₂ O ₃	CaO	MgO	Fe ₂ O ₃	Na ₂ O	SO ₃	TiO ₂
GGBFS	32.19	13.43	41.04	9.40	0.52	-	1.51	0.98
FA	55.12	26.08	5.15	1.28	7.98	0.16	0.77	1.24
OPC	17.65	2.81	68.38	1.75	4.91	-	1.92	0.35

Table 2: Mixture design of AC and OC (kg/m³)

	AC	OC
GGBFS	200	-
FA	200	-
Cement	-	320
SiO ₂	27.5	-
Na ₂ O	18.93	-
Water	153.6	166
Aggregate [0-4 mm]	789.1	836.4
Aggregate [4-8 mm]	439.8	449
Aggregate [8-16 mm]	524.7	564
Liquid/binder	0.5	0.52
Volume ratio of binder/concrete	0.31	0.30

2.2 Experiments

Compressive strength of AC and OC cured for 7 days and 28 days was measured according to NEN-EN 12390-3 (NEN-EN 12390-3 2009).

Drying shrinkage of AC and OC was measured on prism samples (100×100×400 mm³). One group of samples was exposed to drying at 1 day after casting and the other one was exposed at 28 days (1 day in the mould with plastic cover and 27 days in sealed plastic bags). The relative humidity of the environment was 50 ± 0.3%. Three replicates were measured for each mixture exposed at each age and the deviation of the results is less than 10%. The mass changes of the samples were measured with a balance with an accuracy of 0.01 gram.

Shrinkage induced stress in the concrete was examined with the ring test. The depth of the concrete and steel rings was 75 mm. The inner radius of the steel ring was 75 mm, while its

outer radius and the inner radius of the concrete ring were 87.5 mm. The outer radius of the concrete ring was 125 mm (so, its thickness was 37.5 mm). The strain gauges started to record the strain of the inner ring immediately after the concrete was cast in between the steel rings. The ring was then sealed by plastic film to avoid evaporation. One group of rings was sealed for 1 day and the other for 28 days, before the top and the bottom of rings were exposed to drying at the relative humidity of 50% (Hossain and Weiss 2004; Turcry et al. 2006). Since the concrete and the inner ring deform in coordination, the absolute value of the stress detected on the inner ring was identical to the stress generated in the concrete. Two replicates for each mixture under each condition were measured.

3 Results and discussion

3.1 Compressive strength

The measured compressive strength of AC and OC cured for 7 days and 28 days is shown in Table 3. It can be seen that AC showed about 45% higher compressive strength than OC at both ages. This was in good agreement with the literature (Arbi et al. 2015; Prinsse 2017; Wang et al. 1994), where high compressive strength was normally reported for slag and fly ash activated by sodium hydroxide plus sodium silicate. Although the liquid/binder ratio of AC is similar to OC, the microstructures of the two systems are different. In OC, the water content directly reflects the initial porosity, which would of course decrease due to the growth of reaction products surrounding the cement particles and finally percolates to form a porous skeleton (Ye 2003); in AC, however, the activator or the subsequent pore solution contains besides water plenty of alkali and silicate ions, which act not only as reactants but also nucleation sites for the formation of reaction products. Compared with the growth of CSH gels surrounding cement particles, the direct formation of CASH gels in the interstitial space of AC has a much more prominent space-filling effect (Provis et al. 2012; Zuo, Nedeljković, and Ye 2019), which results in a much denser pore structure. As reported in (Li et al. 2017) and (Ye 2016), AASF pastes show very few capillary pores.

Table 3: Compressive strength of AC and OC (MPa)

Compressive strength	AC	OC
7 days	57.5	39.6
28 days	74.0	51.1

Besides the ions in the activator, the high reactivity of the finely ground slag may also contribute to the dense microstructure and consequently the high strength of AC.

3.2 Weight loss

The weight loss results of AC and OC exposed at 1 day and 28 days were shown in Figure 1. It can be observed that the weight loss of AC during drying was much lower than that of OC regardless of the exposure age. The first reason for this was the slightly lower water content in AC compared with OC (153.6 kg/m³ vs. 166 kg/m³), although the difference was small. The second reason was the finer pore structure in AC, where a less amount of water would evaporate in an environment with the same relative humidity (the porosity data was reported previously in (Li et al. 2017; Nedeljkovic et al. 2016)).

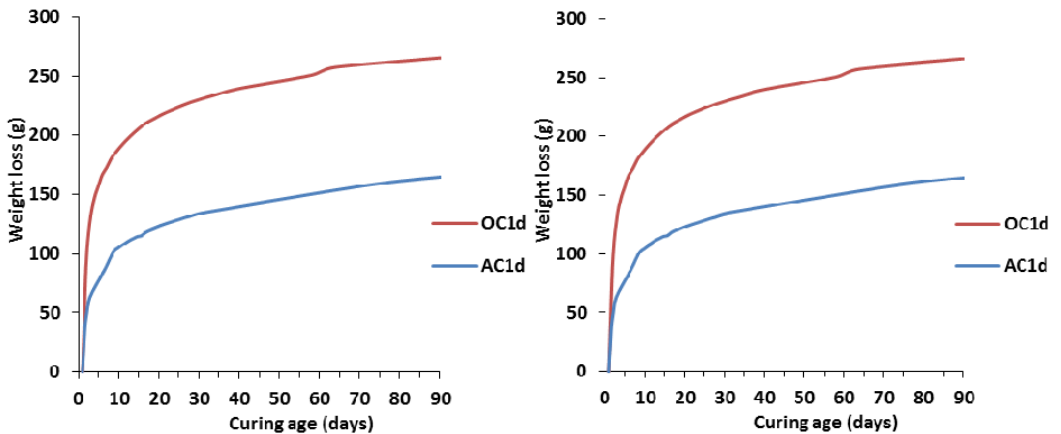


Figure 1: Weight loss of AC and OC exposed at 1 day (a) and 28 days (b)

3.3 Drying shrinkage

The drying shrinkage of AC and OC exposed at 1 day and 28 days (entitled as AC1d, OC1d, AC28d and OC28d, respectively) is shown in Figure 2.

It can be seen that the drying shrinkage of AC was much higher than OC when the samples were subjected to drying at 1 day after casting, although the water loss of AC was lower. This indicates that AC was more susceptible to the drying, which is consistent with the finding from (Thomas, Lezama, and Peethamparan 2017). The drying shrinkage results correspond well with the results from (Palacios and Puertas 2007). The first reason for the high drying shrinkage of AC was the high capillary pressure in AC in the early age. AASF binders were well known to generate severe self-desiccation and high autogenous

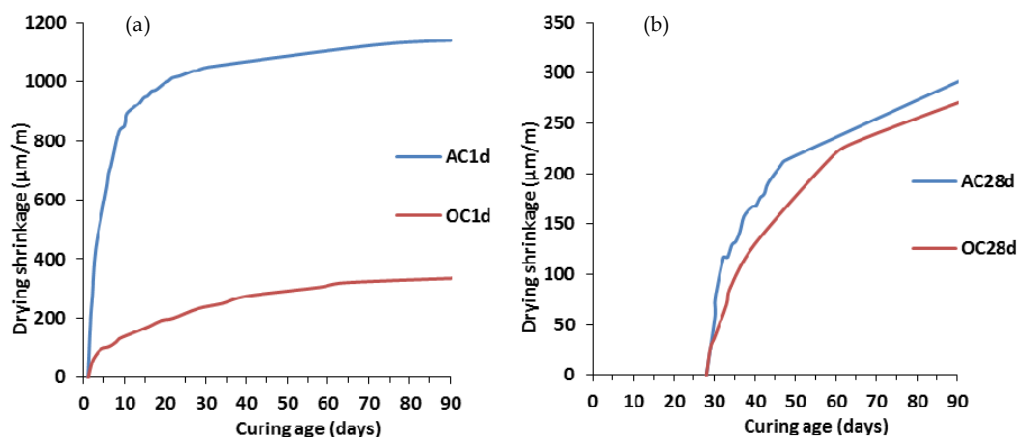


Figure 2: Drying shrinkage of AC and OC exposed at 1 day (a) and 28 days (b)

shrinkage in the early age (Li et al. 2017; Uppalapati and Cizer 2017). When the concrete was exposed at one day after casting, the drying occurred from the surface while the self-desiccation developed severely inside, resulting in a low average relative humidity and hence a high capillary pressure in AC (Kumarappa, Peethamparan, and Ngami 2018). Another factor contributed to the high drying shrinkage of AC was the large saturation fraction in AC. Saturation fraction is the ratio between the evaporable water content and the total pore volume, and it determines how large fraction of solid was under the load of capillary pressure, according to (Bentz, Garboczi, and Quenard 1998). Since AC had similar total water content ($153.6 \text{ kg}/\text{m}^3$ vs. $166 \text{ kg}/\text{m}^3$) but much lower water loss during drying (see Figure 1) compared with OC, AC was supposed to have a higher saturation fraction, which contributed to a larger deformation. Besides capillary pressure and saturation fraction, the non-elastic deformability of the gel is also an important parameter responsible for the early age drying shrinkage (Ye and Radlińska 2016). In the current concrete where the slag to fly ash ratio is 1, the CASH type gels were the dominant gels (Ismail et al. 2014; Nedeljković et al. 2016). It was reported in the literature that the CASH gels exhibit pronounced viscous characteristics due to rearrangement and reorganization of the gels (Ye and Radlińska 2016) and AC exhibits much higher creep coefficient than OC in the early age (Kostiuchenko, Liu, and Aldin 2018; Li, Kostiuchenko, and Ye 2018). That means a much larger deformation would be generated in AC even under the same force as OC.

After stored in sealed condition for 28 days, AC exhibited similar drying shrinkage with OC, as shown in Figure 2 (b). This actually is positive information for the acceptance of AC

in engineering applications. Before subjected to drying at 28 days, the autogenous shrinkage of AC had sufficiently developed and therefore the increment of the capillary pressure in AC after exposure to drying was not so significant compared with the case where AC was exposed at the first day. Hence, the drying shrinkage of AC exposed at 28 days reached only 290 $\mu\text{m}/\text{m}$, which was comparable with the one of OC.

3.4 Shrinkage-induced stress

3.4.1 Stress in AC and OC exposed at 1 day

The stress developments in AC and OC exposed at 1 day (entitled as AC1d and OC1d, respectively) were compared in Figure 3. Since visible cracks were already observed on the top surface of the AC ring after drying for 28 days, the stress of AC was measured till that time. No cracking was observed for OC in the period of 90 days.

As shown in Figure 3, the stress generated in AC developed much faster than in OC in the first 3 days, which was consistent with the higher early age drying shrinkage of AC as discussed in section 3.3. The stress in AC at 3 days reached 3.4 MPa, which was more than 3 times higher than the stress in OC at the same age. However, after that time, the stress in AC dramatically decreased, reaching around only 1 MPa at 1 month of drying, while the stress in OC kept increasing reaching around 6 MPa.

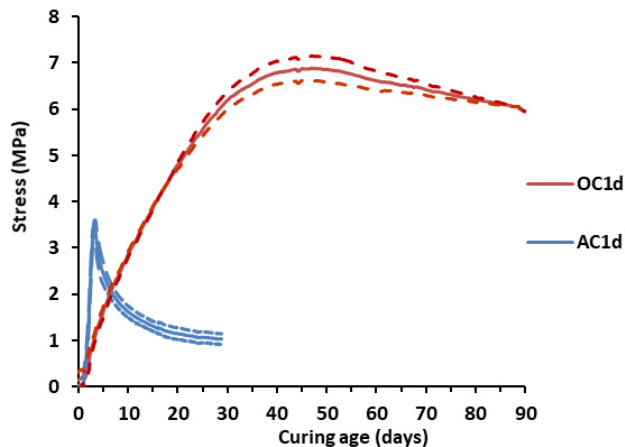


Figure 3: Shrinkage-induced stress in AC and OC. The concrete was sealed in the first day after casting and exposed after that. The average stress is shown in solid line while the results of the two replicates are shown in dashed lines.

The sudden decrease of the stress in AC was probably due to the development of micro- to macro- cracking (Lura, Jensen, and Weiss 2009), although thorough cracking was not observed in AC1d. In fact, the development of microcracking due to shrinkage has been intensively reported in the literature for slag based alkali-activated materials (Collins and J. G. Sanjayan 2000; Li et al. 2019; Nedeljković et al. 2018). For AC1d, microcrack occurred and had developed to form macro cracking on the top surface of the concrete ring, as shown in Figure 4. In contrast, no visible cracking was found on the bottom surface although it was exposed at the same time as the top surface, as shown in Figure 5. This discrepancy may be due to the segregation before setting, i.e. more aggregates settled to the bottom side of the ring under the gravity force, resulting in a relatively stronger part in the bottom and a weaker part in the top surface. The exposed aggregates observed on the bottom side of AC ring, as shown in Figure 5, was due to spalling of the covering paste during demoulding, when some paste got stuck to the bottom steel board resulting from the insufficient demoulding oil applied in advance. According to our further trails and

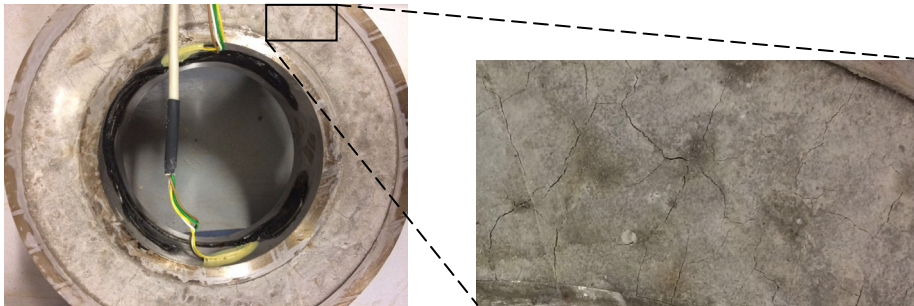


Figure 4: The top surface of AC1d. The concrete was sealed in the first day after curing and exposed after that. Cracking was observed on the top surface at the age of 1 month.

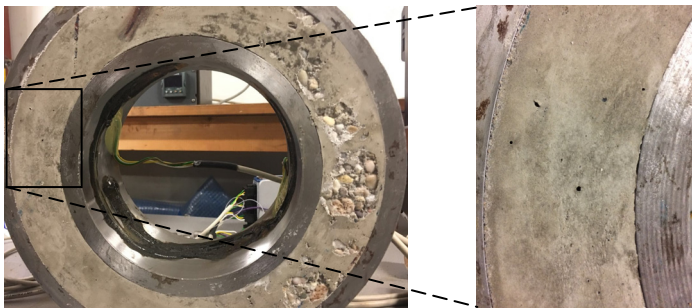


Figure 5: The bottom surface of AC1d. The concrete was sealed in the first day after curing and exposed after that. No cracking was observed at the age of 1 month.

experiences, we would like to suggest the AAMs researchers to use Vaseline as demoulding agent instead of the common oil developed for OPC, since Vaseline better resists alkalis and thus better separates the AAMs and the steel (e.g. rings and other kinds of moulds).

As indicated by Figure 4 and 5, the cracks observed on the ring of AC were not fully connected in the cross-section, so that the concrete did not completely fail. However, the cracks were large enough to harm the mechanical properties and can also form preferential continuous pathways for mass transport and chemical attacks, thus should be avoided in engineering.

3.4.2 Stress in AC and OC exposed at 28 days

The stress developments in AC and OC exposed at 28 days (entitled as AC28d and OC28d, respectively) were presented in Figure 6.

In the first 28 days, the stress in AC was much higher than in OC due to the large autogenous shrinkage of AC in this period (Li et al. 2018). After exposure to drying, the stresses in OC and AC both developed rapidly, reaching 6-8 MPa at the age of 38 days (10 days of drying). This was consistent with the drying shrinkage developments of these two concretes as described in section 3.3. After that, however, the stress in AC began to

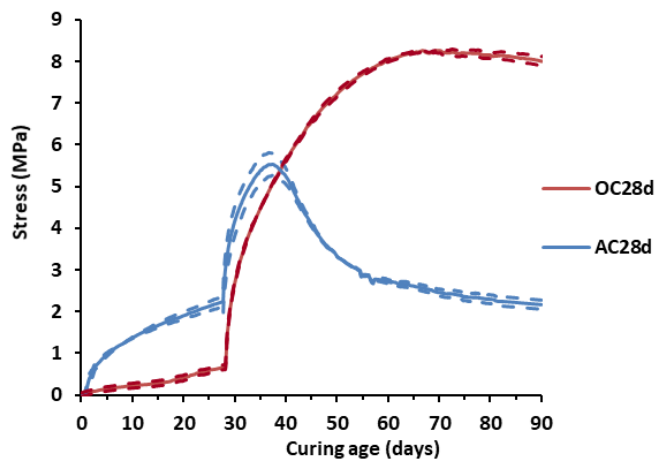


Figure 6: Shrinkage-induced stress in AC and OC. The concrete was sealed in the first 28 days after casting and exposed after that. The average stress is shown in solid line while the results of the two replicates are shown in dashed lines.

decrease to less than 3 MPa, which was even lower than the stress before drying. This gradual decrease was believed to be due to stress relaxation. As mentioned previously, CASH gels, the main reaction products in AC, exhibit pronounced viscoelasticity (Ye and Radlińska 2016). From the deformation point of view, the pronounced viscoelasticity induces significant creep, as discussed in the previous section; while from the force point of view, it means great relaxation, as in the case that the concrete restrained by the steel ring (Neville 2011). Thanks to the relaxation, AC28d did not crack in the period studied, otherwise, if the stress kept increasing at a high rate it would probably surpass the tensile strength of AC and lead to cracking. Of course, OPC systems are also not purely elastic, as indicated by the stress decrease in OC1d at the age of 48 days and in OC28d at the age of 68 days, but the relaxation of stress in OC was much less significant compared to AC. As a result, the shrinkage-induced stress in AC1d and AC28d became much lower than in OC.

According to Table 3, AC showed much higher compressive strength than OC, so the tensile strength of AC should also be higher than OC due to the linear relation between tensile and compressive strength (Neville 2011). Even though the real tensile strength of the concrete under sealed and restraint conditions may not be the same as in humid and free condition, the tensile strength of AC was supposed to be not lower than OC. In contrast, the tensile stress in AC28d was only one-quarter of the stress in OC28d at 90 days. Therefore, it could be inferred that the long-term cracking potential of AC should be lower than OC if the samples were cured in sealed condition for 28 days before subjected to drying. The time with the highest cracking potential of AC seems to lie in the drying age of around 10 days when the shrinkage-induced stress reached the maximum.

4 Final remarks

According to the results above, cracks were observed on sample AC1d but not on sample OC1d. However, it is inappropriate to conclude that AC has higher cracking tendency than OC due to early age drying, because the strengths of the compared concretes were largely different. Although the binder to aggregate volume ratio and the liquid to binder ratio were kept rather similar for the two concretes, AC generated 45% higher compressive strength than OC. One key reason behind the different strengths is the much denser microstructure of AC, as discussed in section 3.1. Dense pore structure, on one hand, means high strength but on the other hand, means small diameters of the meniscus and consequently severe shrinkage during self-desiccation or drying due to exposure (Lura,

Jensen, and Van Breugel 2003). Therefore, using OC with much lower strength and coarser pore structure as the reference is insufficient to draw conclusions on whether AC has a high or low cracking tendency. Future research on comparing the drying shrinkage of AC and OC with similar strength level is needed to better evaluate the cracking tendency of AC by reference to OC, although in that case, the liquid to binder ratio of the OC should be inevitably lower than the studied AC to provide the required strength.

5 Conclusions

- With similar binder content and liquid/binder ratio, alkali-activated blast furnace slag and fly ash concrete (AC) showed a 45% higher compressive strength than ordinary Portland cement concrete (OC).
- The weight loss of AC was less than that of OC regardless of the exposure age.
- The drying shrinkage of AC was much higher than OC if the samples were dried from 1 day after casting, but if the samples were stored in sealed condition for 28 days beforehand, the subsequent drying shrinkages of AC and OC were comparable.
- Despite the exposure age, the stresses generated in AC developed faster than in OC at the beginning, but experienced great relaxation after certain ages, reaching much lower values than in OC in the long term.
- For AC exposed at 1 day, small cracks were observed on the top surface of the concrete ring. Therefore, protecting AC from drying at an early age is recommended to avoid micro or macrocracking.
- If the concrete was sealed for 28 days before drying, AC seems to have a lower cracking tendency than OC due to relaxation.
- Vaseline is suggested to be used as the demoulding agent for AC. Traditionally used demoulding oil for OPC can be ineffective for AAMs.

Acknowledgments

This work is supported in part by the scholarship from China Scholarship Council (CSC). Marija Nedeljković at Microlab of the Delft University of Technology is acknowledged for discussions on the mixture design and demoulding agent.

References

- Arbi, K., M. Nedeljkovic, Y. Zuo, S. Grünewald, A. Keulen, and G. Ye. 2015. "Experimental Study on Workability of Alkali Activated Fly Ash and Slag-Based Geopolymer Concretes." *Geopolymers: The Route to Eliminate Waste and Emissions in Ceramic and Cement Manufacturing*. ISBN: 9781326377328 75–78.
- Arbi, Kamel, Marija Nedeljković, Yibing Zuo, and Guang Ye. 2016. "A Review on the Durability of Alkali-Activated Fly Ash/Slag Systems: Advances, Issues, and Perspectives." *Industrial & Engineering Chemistry Research* 55(19):5439–53.
- Bentz, Dale P., Edward J. Garboczi, and Daniel A. Quenard. 1998. "Modelling Drying Shrinkage in Reconstructed Porous Materials: Application to Porous Vycor Glass." *Modelling and Simulation in Materials Science and Engineering* 6(3):211.
- Burciaga-Díaz, Oswaldo, Jose Ivan Escalante-García, Raúl Arellano-Aguilar, and Alexander Gorokhovskiy. 2010. "Statistical Analysis of Strength Development as a Function of Various Parameters on Activated Metakaolin/Slag Cements." *Journal of the American Ceramic Society* 93(2):541–47.
- Cartwright, Christopher, Farshad Rajabipour, and Aleksandra Radli. 2014. "Shrinkage Characteristics of Alkali-Activated Slag Cements." *Journal of Materials in Civil Engineering* 27(7):1–9.
- Collins, Frank and Jay G. Sanjayan. 2000. "Effect of Pore Size Distribution on Drying Shrinking of Alkali-Activated Slag Concrete." *Cement and Concrete Research* 30(9):1401–6.
- Collins, Frank and Jay G. Sanjayan. 2000. "Cracking Tendency of Alkali-Activated Slag Concrete Subjected to Restrained Shrinkage." *Cement and Concrete Research* 30(5):791–98.
- Douglas, E., A. Bilodeau, J. Brandstetr, and V. M. Malhotra. 1991. "Alkali Activated Ground Granulated Blast-Furnace Slag Concrete: Preliminary Investigation." *Cement and Concrete Research* 21(1):101–8.
- Hossain, Akhter B. and Jason Weiss. 2004. "Assessing Residual Stress Development and Stress Relaxation in Restrained Concrete Ring Specimens." *Cement and Concrete Composites* 26(5):531–40.
- Ismail, Idawati, Susan A. Bernal, John L. Provis, Rackel San Nicolas, Sinin Hamdan, and Jannie S. J. Van Deventer. 2014. "Modification of Phase Evolution in Alkali-Activated Blast Furnace Slag by the Incorporation of Fly Ash." *Cement and Concrete Composites* 45:125–35.

- Juenger, M. C. G., F. Winnefeld, J. L. Provis, and J. H. Ideker. 2011. "Advances in Alternative Cementitious Binders." *Cement and Concrete Research* 41(12):1232–43.
- Kostiuchenko, Albina, J. Liu, and Zainab Aldin. 2018. "Mechanical Properties and Creep Behavior of an Alkali-Activated Concrete." P. 9 in *Alkali Activated Materials and Geopolymers: Versatile Materials Offering High Performance and Low Emissions*.
- Kumarappa, Ballekere Darshan, Sulapha Peethamparan, and Margueritte Ngami. 2018. "Autogenous Shrinkage of Alkali Activated Slag Mortars: Basic Mechanisms and Mitigation Methods." *Cement and Concrete Research* 109(July 2017):1–9.
- Li, Zhenming, Albina Kostiuchenko, and Guang Ye. 2018. "Autogenous Shrinkage-Induced Stress of Alkali-Activated Slag and Fly Ash Concrete under Restraint Condition." P. 24 in *Alkali Activated Materials and Geopolymers: Versatile Materials Offering High Performance and Low Emissions*, edited by ECI. Tomar.
- Li, Zhenming, Marija Nedeljković, Boyu Chen, and Guang Ye. 2019. "Mitigating the Autogenous Shrinkage of Alkali-Activated Slag by Metakaolin." *Cement and Concrete Research* 122:30–41.
- Li, Zhenming, Marija Nedeljkovic, Yibing Zuo, and Guang Ye. 2017. "Autogenous Shrinkage of Alkali-Activated Slag-Fly Ash Pastes." Pp. 369–72 in *5th International Slag Valorisation Symposium*. Leuven.
- Lura, Pietro, Ole Mejlhede Jensen, and Klaas Van Breugel. 2003. "Autogenous Shrinkage in High-Performance Cement Paste: An Evaluation of Basic Mechanisms." *Cement and Concrete Research* 33(2):223–32.
- Lura, Pietro, Ole Mejlhede Jensen, and Jason Weiss. 2009. "Cracking in Cement Paste Induced by Autogenous Shrinkage." *Materials and Structures/Materiaux et Constructions* 42(8):1089–99.
- Nedeljkovic, Marija, Kamel Arbi, Yibing Zuo, and Guang Ye. 2016. "Physical Properties and Pore Solution Analysis of Alkali Activated Fly Ash-Slag Pastes." *International RILEM Conference on Materials, Systems and Structures in Civil Engineering Conference Segment on Concrete with Supplementary Cementitious Materials* (August).
- Nedeljković, Marija, Kamel Arbi, Yibing Zuo, and Guang Ye. 2016. "Microstructural and Mineralogical Analysis of Alkali Activated Fly Ash- Slag Pastes." in *Microdurability 2016: the International Rilem Conference on Microstructure Related Durability of Cementitious Composites*.

- Nedeljković, Marija, Zhenming Li, and Guang Ye. 2018. "Setting, Strength, and Autogenous Shrinkage of Alkali-Activated Fly Ash and Slag Pastes: Effect of Slag Content." *Materials* 11(11):2121.
- NEN-EN 12390-3. 2009. "Testing Hardened Concrete - Part 3: Compressive Strength of Test Specimens."
- Neville, A. M. 2011. *Properties of Concrete*.
- Neville, Adam. 2003. "Neville On Concrete." *An Examination of Issues in Concrete Practice* 531.
- Palacios, M. and F. Puertas. 2007. "Effect of Shrinkage-Reducing Admixtures on the Properties of Alkali-Activated Slag Mortars and Pastes." *Cement and Concrete Research* 37(5):691-702.
- Prinsse, Silke. 2017. "Alkali-Activated Concrete: Development of Material Properties (Strength and Stiffness) and Flexural Behaviour of Reinforced Beams over Time." Master Thesis.
- Provis, John L. 2014. "Geopolymers and Other Alkali Activated Materials: Why, How, and What?" *Materials and Structures* 47:11-25.
- Provis, John L. and Jannie S. J. Van Deventer. 2009. *Geopolymers: Structures, Processing, Properties and Industrial Applications*. Woodhead, Cambridge, UK.
- Provis, John L., Rupert J. Myers, Claire E. White, Volker Rose, and Jannie S. J. Van Deventer. 2012. "X-Ray Microtomography Shows Pore Structure and Tortuosity in Alkali-Activated Binders." *Cement and Concrete Research* 42(6):855-64.
- Scrivener, Karen L. and R. James Kirkpatrick. 2008. "Innovation in Use and Research on Cementitious Material." *Cement and Concrete Research* 38(2):128-36.
- See, Heather T., Emmanuel K. Attiogbe, and Matthew A. Miltenberger. 2003. "Shrinkage Cracking Characteristics of Concrete Using Ring Specimens." *ACI Materials Journal* 100(3):239-45.
- Thomas, R. J., Diego Lezama, and Sulapha Peethamparan. 2017. "On Drying Shrinkage in Alkali-Activated Concrete: Improving Dimensional Stability by Aging or Heat-Curing." *Cement and Concrete Research* 91:13-23.
- Turcry, Philippe, Ahmed Loukili, Khalil Haidar, Gilles Pijaudier-Cabot, and Abdeldjelil Belarbi. 2006. "Cracking Tendency of Self-Compacting Concrete Subjected to Restrained Shrinkage: Experimental Study and Modeling." *Journal of Materials in Civil Engineering* 18(1):46-54.

- Uppalapati, S. and Ö. Cizer. 2017. "Assessing the Autogenous Shrinkage of Alkali- Activated Slag/Fly Ash Mortar Blends." American Concrete Institute, ACI Special Publication 2017-Janua (SP 320).
- Wang, Shao-Dong, Karen L. Scrivener, and P. L. Pratt. 1994. "Factors Affecting the Strength of Alkali-Activated Slag." *Cement and Concrete Research* 24(6):1033-43.
- Ye, G. 2003. *Experimental Study and Numerical Simulation of the Development of the Microstructure and Permeability of Cementitious Materials*.
- Ye, Hailong. 2016. "Mechanisms and Mitigation of Shrinkage in Alkali-Activated Slag."
- Ye, Hailong and Aleksandra Radlińska. 2016. "Shrinkage Mechanisms of Alkali-Activated Slag." *Cement and Concrete Research* 88:126-35.
- Zuo, Yibing, Marija Nedeljković, and Guang Ye. 2019. "Pore Solution Composition of Alkali-Activated Slag/Fly Ash Pastes." *Cement and Concrete Research* 115(October 2018):230-50.

